Arsenic-bound excitons in diamond

J. Barjon[*] and F. Jomard
Groupe d'Etude de la Matière Condensée, Université Versailles St Quentin & CNRS, 45 Avenue des Etats-Unis, F-78035 Versailles, France

S. Morata
Ion Beam Services, Rue G. Imbert Prolongée, Z. I. Peynier Rousset, F-13790 Peynier, France
(Received 2 August 2013; revised manuscript received 29 October 2013; published 3 January 2014)

A set of new excitonic recombinations is observed in arsenic-implanted diamond. It is composed of two groups of emissions at 5.355/5.361 eV and at 5.215/5.220/5.227 eV. They are respectively attributed to the no-phonon and transverse-optical phonon-assisted recombinations of excitons bound to neutral arsenic donors. From the Haynes rule, an ionization energy of 0.41 eV is deduced for arsenic in diamond, which shows that arsenic is a shallower donor than phosphorus (0.6 eV), in agreement with theory.

DOI: 10.1103/PhysRevB.89.045201 PACS number(s): 71.35.−y, 71.55.Cn, 78.60.Hk, 81.05.ug

In diamond, phosphorus is the only donor reported so far to induce reproducible *n*-type conductivity. The first *p*-*n* junctions made of diamond were grown by chemical vapor deposition (CVD) with phosphorus doping in 2001.[1] However, the phosphorus donor level is very deep, at 0.6 eV below the conduction band minimum.[2] An *n*-type diamond grown with phosphorus impurities is therefore almost insulating at room temperature, with free-electron densities of only $\sim 10^{11}$ cm^{-3} in the best samples.[3,4] This strongly contrasts with *p*-type conduction, which is much more easily obtained in diamond with a boron acceptor level at 0.37 eV above the valence band.

The deep character of the phosphorus donor hinders the development of diamond-based electronic devices, which are highly desired in order to exploit the exceptional properties of diamond as a semiconductor (wide band gap, high carrier mobilities, highest reported breakdown voltage, highest reported thermal conductivity . . .). The unique combination of diamond electronic properties is expected to improve the performances of electronic devices to an ultimate level. That is the reason why the search for shallower donors has been so active during the last decades, though without convincing experimental results. From the theoretical point of view, arsenic and antimony should be single substitutional dopants shallower than phosphorus, with donor levels expected at 0.4 eV and 0.3 eV below the conduction band, respectively.[5] However, the shallow donor character of arsenic in diamond still has no experimental evidence up to now.

The purpose of this paper is to show that arsenic impurities can provide donor centers in diamond. The experimental method is based on ion implantation followed by high-temperature annealing in order to introduce arsenic impurities in the diamond crystal lattice. Their location in substitutional sites is observed by the associated bound exciton recombinations using a high-sensitivity optical system. The experimental conditions are first validated with phosphorus implantation, as evidenced by the energetic signature of phosphorus-bound exciton recombinations, which are well known from *n*-type CVD diamond. In arsenic-implanted samples, new excitonic recombinations are observed and are attributed to neutral-arsenic-donor bound excitons. The energy level of the arsenic donor is estimated on the basis of Haynes law. It indicates that the arsenic level is located at 0.41 eV below the conduction band minimum, which is significantly shallower than phosphorus in diamond.

Implantations were performed on (100)-oriented diamond single crystals. Three of them were 30-μm-thick homoepitaxial layers grown by CVD on Ib high-pressure, high-temperature substrates.[6] These diamond layers were implanted with phosphorus, arsenic, or antimony atoms in the samples identified as P-implant, As-implant1, and Sb-implant. As shown later, these layers were slightly contaminated by boron atoms. This complicated the interpretation of arsenic implantation results, which is the reason why an additional sample was used for arsenic implantation, named As-implant2. It is a two-sided polished, 0.5-mm-thick single crystal purchased from Element6 with extremely low impurity contents (CVD electronic grade). Its boron concentration is guaranteed below 2×10^{14} atoms/cm^3 by the supplier.

Because of the metastability of diamond with respect to graphite, annihilation of implantation defects by annealing is not straightforward in diamond. The pioneered studies of Prawer and Kalish[7] have established that implantation in a diamond target heated at high temperature decreases implantation damage in diamond. The so-called hot implantation method, followed by high-temperature annealing, has recently given encouraging results in the case of *p*-type diamond implanted with boron.[8] The hot implantation is further investigated here with phosphorus, arsenic, and antimony atoms. Box implantation profiles were formed by multiple implantations at different ion energies using the IBS/IMC200 implanter model, previously simulated with SRIM software.[9] The damage defects estimated from the simulation are below the critical concentration of 10^{22} vacancies/cm^3. Above this defect concentration, it has been shown that any atmospheric pressure annealing leads to a graphitization of the implanted region.[10]

The diamond temperature during the ion implantation was 500 °C. The heat treatment after the ion implantation was performed at 1700 °C for 30 min in high-purity Ar (9N). Figure 1 presents the impurity depth profiles in the implanted diamonds as measured by secondary ion mass spectrometry (SIMS) with IMS Cameca 7f equipment. These measurements confirm an almost constant concentration of implanted species at a 120–150 nm depth (box-profiles): 4×10^{19} P/cm^3 for

 ©2014 American Physical Society

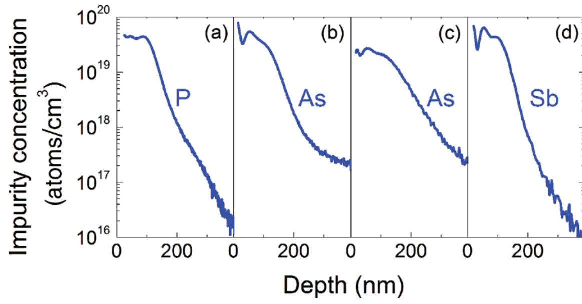

FIG. 1. (Color online) Depth profiles of impurities implanted in the diamond samples as measured by SIMS: (a) P-implant1, (b) As-implant1, (c) As-implant2, and (d) Sb-implant.

P-implant; 4×10^{19} As/cm^3 for As-implant1; 2.5×10^{19} As/cm^3 for As-implant2; and 4×10^{19} Sb/cm^3 for Sb-implant. In all samples, the boron signal was below the SIMS detection limit of 5×10^{15} B/cm^3. The depth profiles were also checked to make sure they showed no evolution after the annealing step.

The exciton recombinations were observed by cathodoluminescence (CL) in the ultraviolet (UV) range. CL spectra were collected before and after the doping process by using an optical detection system from Horiba Jobin Yvon SA, installed on a JEOL7001F field-emission scanning electron microscope (SEM). The samples were mounted on a GATAN cryostat SEM-stage, which was cooled at 5 K with liquid helium. The effective diamond temperature was slightly higher, as shown later. The specimens were coated with an ~5 nm semitransparent gold layer in order to evacuate away electrical charges. Low-energy electrons (7 keV) were chosen to inject carriers in the implanted region. The experiments were performed in weak excitation conditions (beam current ~5 nA), below the nucleation threshold of electron-hole liquid droplets. The CL emission was collected by a parabolic mirror and focused with mirror optics on the entrance slit of a 55 cm focal length monochromator. This achromatic all-mirror optics bench, combined with a suitable choice of ultraviolet (UV) detectors and gratings, provides an excellent sensitivity down to 200 nm. A silicon charge-coupled-display camera was used to record spectra. The use of an 1800 grooves/mm grating provides an energy separation of 0.5 meV at 5.35 eV between two adjacent pixels. CL spectra were calibrated against the 237.83 nm emission line of an Hg-vapor lamp.

The CL spectra of exciton recombinations in the diamond specimens are presented in Fig. 2. The intrinsic features, namely, the three free exciton lines X_{TO}, X_{TA}, and X_{LO}, are observed in all samples, with maxima at 5.27 eV, 5.32 eV, and 5.25 eV, respectively.[11] In indirect band-gap semiconductors such as diamond, the free exciton recombination requires the emission of a phonon to ensure the conservation of momentum ($X \rightarrow h\nu + \hbar\omega$). The transverse optical (TO) phonon is the most efficient assisting phonon in diamond. Longitudinal optical (LO) or transverse acoustical (TA) phonons also assist the free exciton recombination, giving recombinations with similar asymmetrical shapes but less intensity. Their low-energy emission threshold corresponds to the free exciton ground state, with radiation produced by recombining excitons

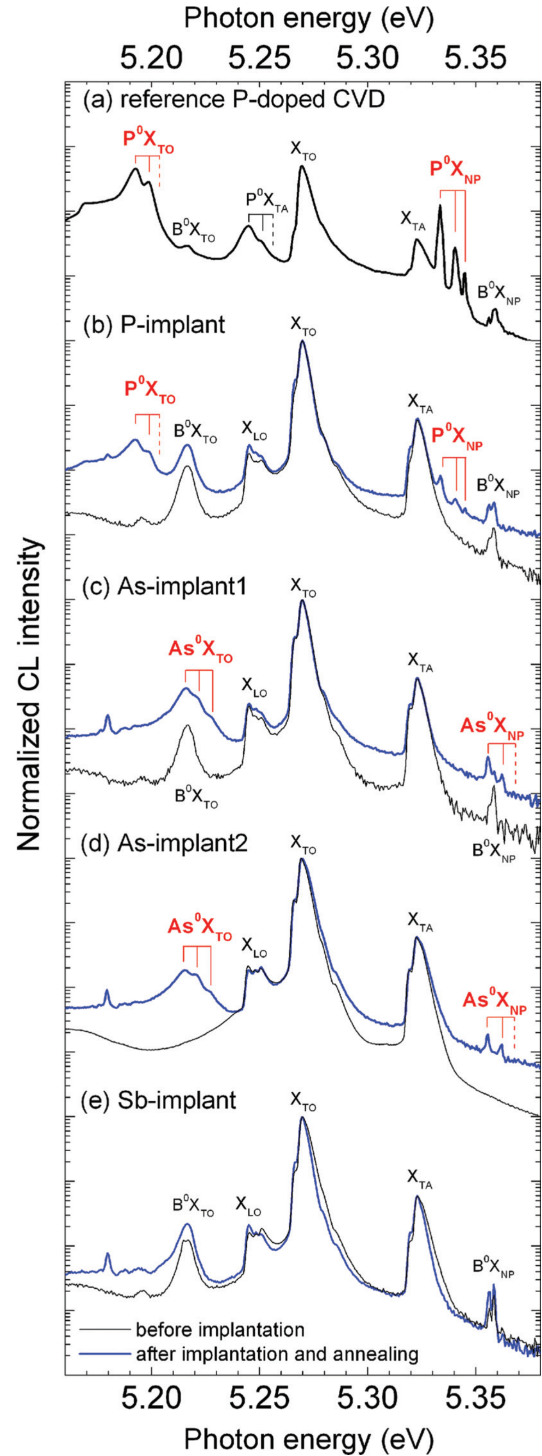

FIG. 2. (Color online) Cathodoluminescence spectra of exciton recombinations in diamond at 20 K. (a) Reference spectrum of an n-type diamond layer grown by CVD with phosphorus impurities.[16] The CL spectra of implanted diamonds are reported before (thin black lines) and after (thick blue lines) hot implantation at 500 °C and subsequent high-temperature annealing at 1700 °C. (b) Phosphorus implantation in a CVD layer. (c) Arsenic implantation in a CVD layer. (d) Arsenic implantation in a high-purity diamond crystal without detectable boron. (e) Antimony implantation in a CVD layer. The spectra are presented as recorded and normalized to the maximum intensity of the TO-phonon-assisted free exciton recombinations, labeled X_{TO}.

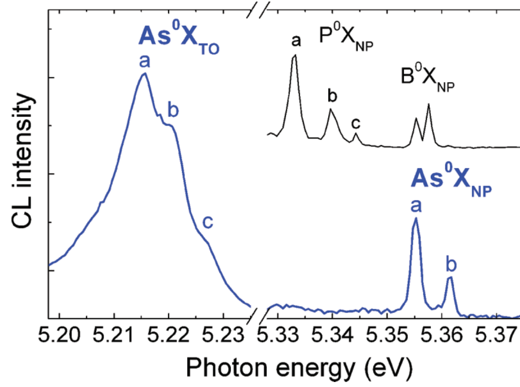

FIG. 3. (Color online) High-resolution CL spectra of the TO and NP neutral arsenic-bound exciton recombinations in As-implant2 (thick blue line). The P^0X_{TO} and B^0X_{NP} recombinations observed in P-implant are added for comparison (thin black line). The high-energy tail of X_{TA} was subtracted from NP recombinations for better clarity.

having zero thermal energy at:

$$h\nu)_X = E_g - E_X - \hbar\omega \tag{1}$$

where E_g is the diamond band gap, E_X the free exciton binding energy, and $\hbar\omega$ is the energy of the TO, TA, or LO assisting phonon. On the other side, the high-energy tails of free exciton recombinations reflect the distribution of exciton kinetic energies.[11] The free exciton gas temperature was then measured from a fit of the high-energy Boltzmann tail to the X_{TO} line. It is found equal to 20 ± 5 K in the reported spectra.

The CL spectra were recorded before and after the full doping process, i.e., implantation and annealing. The exciton recombinations before implantation are first analyzed in the following discussion. The CL spectra of the three homoepitaxial diamond layers reported in Fig. 2, parts (b), (c), and (e), show the free exciton recombinations but also the characteristic recombination energies of excitons that are bound to neutral boron acceptors. The most intense is the B^0X_{TO} peak at 5.216_0 eV, involving the emission of a TO phonon. It is accompanied by weaker and much sharper B^0X recombinations with no phonon (NP),[12,13] observed with a doublet at 5.355_3 and 5.357_6 eV (better resolved in Fig. 3). Contrary to free excitons, we remind the reader that a bound exciton can recombine without phonon emissions: This is because of the localization in the real space of bound excitons around the dopant impurity, which produces an increase of the exciton wave-function extension in k-space. This allows the bound exciton to recombine with NP, though at a lower rate than the TO-assisted recombinations. The measured energy difference between the B^0X_{TO} and the B^0X_{NP} recombinations is about 141 meV. This is the energy of a TO phonon that has a momentum located at k = 0.76 along the [001] direction in the Brillouin zone, where the conduction band is minimum in diamond. These are the characteristics of TO phonons that assist indirect exciton transitions in diamond.[11]

The main features of dopant-bound excitons in diamond could be summarized as follows: (i) dominating TO-assisted recombinations at lower energy than TO-assisted free exciton recombinations, as a consequence of the free exciton binding to the impurity; (ii) weak and narrow line-width emissions from the recombinations without phonon emission (NP), where, in the case of shallow dopants such as P or B, NP recombinations are at higher energy than TO-assisted free exciton recombinations; and (iii) an energy separation between these lines precisely corresponding to the 141 meV assisting TO phonon energy. To be specific with the case of a boron-bound exciton, the recombinations are maximum at:

$$h\nu)_{B^0X} = E_g - E_X - E_{loc}(-\hbar\omega) \tag{2}$$

where E_{loc} is the dissociation energy ($B^0X \rightarrow B^0 + X$) of the bound exciton complex (B^-, h^+, e^-, h^+), also called the localization energy.

The luminescence spectroscopy of bound excitons in indirect band-gap semiconductors is also known as an extremely sensitive tool to measure the dopant concentration in substitutional sites, thanks to the comparison between free and bound exciton recombination intensities.[14, 15] With the high-UV-sensitivity setup used here, the detection limit for B^0X_{TO} corresponds to an acceptor concentration of $1 \times 10^{13}/\text{cm}^3$ in diamond. This is much lower than $5 \times 10^{15}/\text{cm}^3$, the atomic concentration of boron detectable with our SIMS equipment in diamond. Before implantation, the CL spectra of the three diamond layers show that they present a residual boron acceptor concentration of $\sim 5 \times 10^{14}/\text{cm}^3$. On the contrary, in the self-standing diamond As-implant2, B^0X_{TO} could not be detected. This proves that its boron acceptor content is $<1 \times 10^{13}/\text{cm}^3$, in good agreement with the purity certified by the commercial supplier. Without implantation but after a 1700 °C annealing, B^0X_{TO} is not detected in As-implant2 either (experiment done on the back face preserved from ion implantation). This reference experiment discards a possible contamination by boron diffusion or an acceptor activation during the high-temperature treatment, at a level below $1 \times 10^{13}/\text{cm}^3$ in the case of As-implant2.

After phosphorus implantation and annealing, emissions appear in the excitonic recombination region presented in Fig. 2(b): a well-resolved triplet of narrow lines around 5.33 eV and a broader peak at 5.192 eV, also composed of a substructure. A reference n-type CVD diamond,[16] where phosphorus impurities were incorporated during growth, is presented for comparison in Fig. 2(a). The line widths and their energy values accurately match. Table I further compares the P-implant exciton emission energies with data published by another group.[17] The relative spacings of the (a, b, c) fine structure triplet are equal at <1 meV. This leads to a clear attribution of the new lines to neutral phosphorus-bound exciton recombinations, labeled P^0X, with all the general features of bound excitons described previously. It demonstrates that, with the implantation and annealing process used, a fraction of the implanted phosphorus atoms is successfully incorporated in donor sites of the diamond crystal, i.e., in carbon substitutional sites.

The concentration of phosphorus in donor sites produced by implantation and annealing would be $1.6 \times 10^{15}/\text{cm}^3$ from the ratio of free to phosphorus-bound exciton recombination intensities.[15] This value is probably underestimated due to free excitons efficiently recombining in the undoped layer underneath. Whatever happens, the donor concentration

TABLE I. Photon energy of the phosphorus- and arsenic-bound exciton recombinations in diamond.

Sample		P-doped CVD[17]	P-implant1	As-implant1	As-implant2
Assisting phonon	Line label	$h\nu$ (eV)–spacing from line a (meV)	$h\nu$ (eV)–spacing from line a (meV)	$h\nu$ (eV)–spacing from line a (meV)	$h\nu$ (eV)–spacing from line a (meV)
NP	a	5.331	5.333_0	5.355_6	5.355_2
	b	5.338–7	5.339_8–6.8	5.362_0–6.4	5.361_4–6.2
	c	5.342–11	5.344_2–11.2	–	–
TO	a	5.191	5.192_3	5.215_9	5.215_6
	b	5.197–6	5.198_3–6.0	5.221_1–5.2	5.220_6–5.0
	c	–	–	5.227_4–11.5	5.227_1–11.5
TO phonon energy NP_a–TO_a (meV)		140	140.7	139.7	139.6

is above $1.6 \times 10^{15}/\text{cm}^3$ in the P-implant sample. We then applied these conditions to the arsenic doping of diamond.

After arsenic implantation and annealing, new emissions appear in the CL spectra of the excitonic region. In the spectrum of As-implant1 [Fig. 2(c)], these are narrow lines around 5.36 eV and a broader peak with a maximum at 5.215 eV. The high-energy narrow lines are distinct from the B^0X_{NP} due to boron contamination. Compared to B^0X_{TO}, the 5.215 eV peak is four times more intense and has a different shape, but its energy at the peak maximum is very close. That is the reason why the high-purity sample As-implant2, without detectable boron acceptors before and after annealing, was necessary to confirm the results obtained with As-implant1. After arsenic implantation and annealing of As-implant2 [Fig. 2(d)], the new narrow lines around 5.36 eV and the broader peak at 5.215 eV are again observed. The two groups of lines are separated by a 140 meV energy (Table I), corresponding to the assisting TO phonon energy. As described in detail for boron and phosphorus previously, these observations precisely match the characteristics of bound exciton transitions in diamond. From that, we conclude that we are in the presence of a new bound exciton in diamond resulting from the arsenic implantation. The recombination energies are reported in Table I. They are clearly different from the one obtained with the phosphorus implantation, showing that they are specific to the arsenic impurity.

On the contrary, with antimony implantation in similar conditions, optical transitions with bound-exciton features do not appear [Fig. 2(e)]. This further highlights that the new bound excitons we observe in As-implanted samples are specific to the As impurity. Note that a narrow line at 5.18 eV also appears in As-, P-, and Sb-implanted samples. This line is thus not specific to the chemical nature of the implanted impurity. Without excitonic characteristics, it is more probably associated to a deep-level emission coming from a defect induced by implantation damage, or related complexes formed under annealing.

In the following paragraphs, we discuss why the donor character of arsenic is clearly indicated by the ground state fine structure of the associated bound-exciton recombinations. It has to be stressed that the splitting of exciton ground states is unusually large in diamond with respect to other semiconductors. The origin of exciton fine structures has been debated intensively and is still not fully elucidated today.[13,18,19,20] However, it is a matter of fact that it provides a signature of the impurity involved in the bound-exciton complexes in diamond. In particular, it seems clear that the 2 meV ground state splitting of boron-bound excitons (doublet shown in Fig. 3) is directly associated with the 2 meV split ground state of isolated neutral boron acceptors in diamond.[13] Such a splitting is not observed in phosphorus donor–bound excitons, nor in the As implants [Fig. 3(b)], excluding the possibility of confusion with boron acceptors.

Figure 3 presents a high-resolution spectrum of the new bound-exciton recombinations related to arsenic implantation. As in the case of boron or phosphorus, the arsenic-bound exciton presents a fine structure splitting. Their a and b components are particularly well resolved in the NP recombinations and repeated 140 meV below in the TO-assisted recombination with an almost constant spacing (cf. Table I). Though not detected in NP-lines, probably because of a much weaker intensity, a third component c is also observed in the TO-assisted recombination at about 11 meV above component a. The (a, b, c) fine structure of arsenic-related bound excitons appears very close to the one of neutral phosphorus–bound excitons, as can be seen in Fig. 3 and Table I. Their line widths and relative intensities b/a are very close, indicating a comparable thermal activation. The similarity of the recombination structures for As and P strongly suggests that the atomic defect introduced by arsenic implantation and annealing in diamond has a donor character.

Moreover, the implantation and annealing process used in this work has proven its ability to introduce substitutional phosphorus in the diamond lattice. It is also likely to be the case for the introduction of arsenic in carbon substitutional sites. In diamond, excitons bind to dopants only if the dopant state of charge is neutral, since excitons bound to ionized dopants are unstable for carrier effective-mass ratios $0.43 < m_e/m_h < 2.33$.[21] The new exciton recombinations observed in As-implanted diamonds are more precisely identified as excitons bound to neutral arsenic donors.

Finally, it is remarkable that the NP and TO recombinations of arsenic-bound excitons are systematically shifted at higher energies compared to the phosphorus case. This means that the localization energy E_{loc} of excitons on arsenic is smaller than on phosphorus. This energy E_{loc} is precisely measurable from the CL spectra according to Eq. (1) and (2): It is the energy difference between the lowest energy component a of the As^0X_{TO} emission and the low-energy threshold of the X_{TO} recombination at 5.265 eV. E_{loc}(As) is found to be equal to 49.6 meV for As-implant2. The same procedure is applied to

phosphorus-implanted diamond, where $E_{loc}(P) = 72.7$ meV. The Haynes empirical law[22] states that the exciton localization energy E_{loc} is proportional to the ionization energy E_i of the dopant. With the established value of $E_i(P) = 0.6$ eV,[2] we find that, $E_{loc} = 0.12E_i$ for phosphorus in diamond. Donors in silicon follow the same relationship ($E_{loc} = 0.12E_i$ in Ref. 22), indicating that the Haynes rule is also valid in diamond. Applying the Haynes rule for donors in diamond, we deduce a 0.41 eV ionization energy for arsenic, which is significantly shallower than for phosphorus. This value is in good agreement with the theoretical predictions of 0.4 eV for single substitutional arsenic by Sque *et al.*[5] Shallower than phosphorus, the arsenic donor in diamond appears to be extremely promising in the route towards semiconductor devices with ultimate performances.

Because our approach is based on an optical detection of the arsenic donor activity, the next step will be the search for a confirmation of the 0.41 eV ionization energy by Hall effect electrical measurements on high-quality diamonds doped with arsenic. This kind of sample is not yet available. The implantation technique has been essential here to experimentally show the shallow donor character of arsenic in diamond. However, it probably creates too many defects compared with the number of arsenic atoms in donor sites to induce efficient n-type conductivity. This work is rather expected to motivate researches on the elaboration of high-quality diamond with arsenic atoms incorporated during growth, by homo-epitaxy for instance.

The authors are grateful to O. Brinza, A. Tallaire, and J. Achard from LSPM-CNRS Villetaneuse, France, for having provided diamond layers, Marie-Amandine Pinault-Thaury for the growth of reference n-type diamond, C. Vilar for essential technical assistance on SEM-CL experiments, L. Ottaviani from IM2NP-CNRS Marseille, France, for providing the high-temperature annealing service, and J. Chevallier for fruitful discussions and a critical reading of the manuscript. The French FUI projects DIAMONIX (08 2 90 6066) and DIAMONIX2 (F1110024M) are acknowledged for their financial support.

---

*julien.barjon@uvsq.fr

[1] S. Koizumi, K. Watanabe, M. Hasegawa, and H. Kanda, Science **292**, 1899 (2001).
[2] E. Gheeraert, N. Casanova, S. Koizumi, T. Teraji, and H. Kanda, Diam. Relat. Mater. **10**, 444 (2001).
[3] S. Koizumi, T. Teraji, and H. Kanda, Diam. Relat. Mater. **9**, 935 (2000).
[4] I. Stenger, M.-A. Pinault-Thaury, T. Kociniewski, A. Lusson, E. Chikoidze, F. Jomard, Y. Dumont, J. Chevallier, and J. Barjon, J. Appl. Phys. **114**, 73711 (2013).
[5] S. J. Sque, R. Jones, J. P. Goss, and P. R. Briddon, Phys. Rev. Lett. **92**, 017402 (2004).
[6] F. Silva, J. Achard, O. Brinza, X. Bonnin, K. Hassouni, A. Anthonis, K. De Corte, and J. Barjon, Diam. Relat. Mater. **18**, 683 (2009).
[7] S. Prawer and R. Kalish, Phys. Rev. B **51**, 15711 (1995).
[8] N. Tsubouchi, M. Ogura, N. Mizuochi, and H. Watanabe, Diam. Relat. Mater. **18**, 128 (2009).
[9] J. F. Ziegler, J. P. Biersack, and U. Littmark, *The Stopping and Range of Ions in Solids* (Pergamon, New York, 1985).
[10] C. Uzan-Saguy, C. Cytermann, R. Brener, V. Richter, M. Shaanan, and R. Kalish, Appl. Phys. Lett. **67**, 1194 (1995).
[11] P. J. Dean, E. C. Lightowlers, and D. R. Wight, Phys. Rev. **140**, A352 (1965).
[12] J. Sharp, A. T. Collins, G. Davies, and G. S. Joyce, J. Phys.: Condens. Matter **9**, L451 (1997).
[13] R. Sauer, H. Sternschulte, S. Wahl, K. Thonke, and T. R. Anthony, Phys. Rev. Lett. **84**, 4172 (2000).
[14] J. Barjon, T. Tillocher, N. Habka, O. Brinza, J. Achard, R. Issaoui, F. Silva, C. Mer, and P. Bergonzo, Phys. Rev. B **83**, 073201 (2011).
[15] J. Barjon, M.-A. Pinault, T. Kociniewski, F. Jomard, and J. Chevallier, Phys. Status Solidi A **204**, 2965 (2007), and references therein.
[16] M.-A. Pinault-Thaury, B. Berini, I. Stenger, E. Chikoidze, A. Lusson, F. Jomard, J. Chevallier, and J. Barjon, Appl. Phys. Lett. **100**, 192109 (2012).
[17] N. Teofilov, R. Sauer, K. Thonke, and S. Koizumi, Physica B **340–342**, 99 (2003).
[18] M. Cardona, T. Ruf, and J. Serrano, Phys. Rev. Lett. **86**, 3923 (2001).
[19] R. Sauer and K. Thonke, Phys. Rev. Lett. **86**, 3924 (2001).
[20] R. Sauer, N. Teofilov, K. Thonke, and S. Koizumi, Phys. Status Solidi A **201**, 2405 (2004).
[21] I. Pelant and J. Valenta, *Luminescence Spectroscopy of Semiconductors* (Oxford University Press Inc., New York, 2012), Chap. 7.
[22] J. R. Haynes, Phys. Rev. Lett. **4**, 361 (1960).